ELSEVIER

Applied Catalysis B: Environmental 32 (2001) 83–94

APPLIED CATALYSIS B: ENVIRONMENTAL

www.elsevier.com/locate/apcatb

Structure sensitivity and in situ activation of benzene combustion on Pt/Al_2O_3 catalysts

T.F. Garetto, C.R. Apesteguía*

Instituto de Investigaciones en Catálisis y Petroquímica (INCAPE), UNL-CONICET, Santiago del Estero 2654, 3000 Santa Fe, Argentina

Received 2 June 2000; received in revised form 1 December 2000; accepted 19 December 2000

Abstract

The structure sensitivity and in situ activation of benzene combustion on Pt/Al_2O_3 catalysts of different platinum and chlorine loadings were studied. The catalyst activities were evaluated through both conversion versus temperature (light-off curves) and conversion versus time catalytic tests. The light-off curves shifted to lower temperature with increasing Pt particle size, thereby suggesting that benzene combustion is a structure sensitive reaction. Kinetically-controlled catalytic tests confirmed that benzene oxidation turnover rates are preferentially promoted by larger Pt crystallites. Kinetic studies showed that the reaction orders and the apparent activation energy are not changed by changing the metallic dispersion. Results are explained by considering that benzene oxidation proceeds via a Langmuir–Hinshelwood mechanism which involves the rapid and strong adsorption of benzene on metallic platinum and assumes that the rate constant of oxygen adsorption is very low compared to the rate constant of the surface reaction. The number of Pt–O bonds of lower binding energy, i.e. the site density of more reactive surface oxygen, increases on larger Pt particles. Low-conversion catalytic tests performed at constant temperature showed that on well-dispersed Pt/Al_2O_3 catalysts the benzene conversion increases with time, irrespective of the chlorine content on the sample. TEM examination and hydrogen chemisorption measurements suggested that the activity increase parallels a concomitant increase in the platinum particle size. In contrast, sintered samples (platinum dispersions lower than 10%) did not exhibit initial activation periods. It is proposed that the initial in situ activation of well-dispersed Pt catalysts is caused by the sintering of the metallic phase. Hot-spots on the metallic particles together with the presence of gaseous water cause the formation of larger Pt crystallites, even at mild reaction conditions. As a result, the benzene conversion increases with time until the formation of larger steady state Pt particles is completed.

Keywords: Benzene combustion; Platinum catalysts; Structure-sensitive reactions

1. Introduction

Catalytic combustion is one of the most important air pollution control technology for eliminating volatile organic compounds (VOCs) present at low concentrations in effluent streams [1,2]. Noble metal catalysts are very active for promoting oxidation reactions and are preferentially used in commercial practice in spite of their cost. Particularly, platinum or palladium supported on alumina carriers are widely employed for the combustion of non-halogenated VOCs [3,4]. Excepting for palladium in the case of methane, platinum is recognized to be the most active metal for hydrocarbon oxidation [5,6]. Platinum-based catalysts have been efficiently employed in the abatement of aromatic hydrocarbons from gaseous or liquid

* Corresponding author. Tel.: +54-342-4555279; fax: +54-342-4531068.
E-mail address: capesteg@fiqus.unl.edu.ar (C.R. Apesteguía).

0926-3373/01/$ – see front matter
PII: S0926-3373(01)00128-X

streams [7–10]. Benzene, toluene, and xylenes (BTX) are usually present in emissions due to solvent evaporation, coating operations, and thermal degradation of plastic materials. Because of its high toxicity, benzene allowable emission levels are significantly lower compared to other VOCs.

In previous work, it has been observed that palladium and platinum catalysts are often activated on stream, ab initio of the hydrocarbon combustion reaction. This phenomenon have been widely studied on palladium-based catalysts; in the case of methane oxidation, several authors have proposed that the initial activation period is caused by reoxidation from Pd metal or oxygen-deficient PdO_{1-x} to more active steady state PdO species [11,12]. In contrast, very few papers have been published using platinum-based catalysts [13,14] and the causes of induction periods on platinum remain unclear. A similar explanation than that proposed above for Pd catalysts is unlikely because there is a general agreement that hydrocarbon oxidation reactions over platinum occur on metallic sites [15].

On the other hand, the effect of varying the platinum particle size on the catalytic combustion of different hydrocarbons has been extensively studied [16–23]. Nevertheless, the results obtained are conflicting, probably due to the fact that the correlation between catalytic activity and metallic dispersion depends on the type of hydrocarbon to be abated. Most of papers on light alkanes combustion, namely methane [16–18], propane [13], butane [19] and heptane [20], have reported that alkane oxidation turnover rates increase with increasing platinum particle size. In contrast, in a recent study on the C_2H_4 combustion over platinum-supported catalysts Pliangos et al. [21] proposed that turnover frequency (TOF) changes, which cannot be explained by structure sensitivity considerations, are caused by interactions between the metal crystallites and the carrier. Very few papers deal with the structure sensitivity of BTX hydrocarbon combustion on Pt-based catalysts. Papaefthimiou et al. [22] studied the oxidation of benzene over Pt-based catalysts. They found that on Pt–Al_2O_3 turnover rates strongly increase with increasing Pt particle size, while on Pt/SiO_2 and Pt/TiO_2, the effect of Pt dispersion is rather weak.

In this work, the oxidation of benzene was studied over a set of Pt/Al_2O_3 catalysts of different metallic dispersion and chlorine concentration. Our aims were to establish the causes of initial activation periods and to obtain further information on the sensitivity of benzene oxidation turnover rates to Pt crystallite size.

2. Experimental

2.1. Catalyst preparation

Five Pt/Al_2O_3 catalysts of different platinum and chlorine contents were prepared. Catalysts I-A and III were made by impregnation at 303 K of a high-purity γ-Al_2O_3 powder (Cyanamid Ketjen CK300) with an aqueous solution of chloroplatinic acid $H_2PtCl_6{\cdot}6H_2O$ (Aldrich, 99.995%) and HCl. The CK300 alumina has BET surface area of $180\,m^2\,g^{-1}$, pore volume of $0.49\,cm^3\,g^{-1}$ and contains 50 ppm sulfur. After impregnation, samples were dried 12 h at 393 K and heated in air stream to 773 K. Then, the chlorine content was regulated using a gaseous mixture of HCl, water and air. Finally, the samples were purged with N_2 and reduced in flowing H_2 for 4 h at 773 K. A portion of catalyst I-A was treated for 2 h in a 2% O_2/N_2 mixture at 858 K in order to sinter the metallic fraction and then reduced 4 h at 773 K; the resulting sintered catalyst is identified here as catalyst I-B. Catalyst II was made following the same procedure used for preparing catalysts I-A and III, and then submitted to a sintering treatment in a 2% O_2/N_2 mixture at 893 K for 4 h. Chlorine-free catalyst F was prepared by impregnation at 303 K of CK300 alumina with an aqueous solution of tetraamine platinum nitrate $Pt(NH_3)_4(NO_3)_2$ (Alfa) for 6 h. The impregnated alumina was dried overnight at 393 K, then heated in air at 773 K for 4 h and finally reduced 4 h at 773 K in hydrogen.

2.2. Catalyst characterization

The platinum dispersion (D) was determined by irreversible H_2 chemisorption. The volumetric adsorption experiments were performed at 298 K in a conventional vacuum instrument equipped with an MKS Baratron pressure gauge. The pressure range of isotherms was 0–0.35 atm (1 atm = 101.3 kPa). Catalysts were outgassed at 773 K in a vacuum of 8×10^{-8} atm and then reduced in H_2 at 573 or 773 K

for 2 h. After cooling to room temperature a first isotherm (primary isotherm) was drawn for measuring the total H_2 uptake. Then, and after 1 h of evacuation at room temperature, a second isotherm (secondary isotherm) was performed to determine the amount of weakly adsorbed H_2. The amount of irreversibly held H_2, $(HC)_i$, was calculated as the difference between total and weakly adsorbed H_2. A stoichiometric atomic ratio $(HC)_i/Pt_s = 1$, where Pt_s implies a Pt atom on surface, was used to calculate the platinum dispersion.

Platinum loadings were measured by atomic absorption spectrometry, whereas chlorine contents on the catalysts were determined by chemical analysis using conventional colorimetric techniques. The metallic phase was examined by transmission electron microscopy (TEM) in a JEOL 100 CX microscope operating at 100 kV. An extractive replica technique was used to prepare the samples [23].

2.3. Benzene oxidation reaction studies

The oxidation of benzene (Merck, 99.7%) was carried out at 1 atm in a fixed-bed tubular reactor (pyrex, 0.8 cm i.d.). Catalyst samples were held as a thin layer above a plug of acid-washed quartz wool. Temperatures were measured using a K-type thermocouple placed into the catalyst bed. Samples were sieved and fraction 0.35–0.42 mm was separated and loaded to the reactor. In standard runs, catalyst loadings (W) of 0.4 g and contact times (W/F^0_{Bz}) of 50 g catalyst h mol^{-1} benzene were used. The reactant was delivered by a syringe pump and vaporized in a 10% O_2/N_2 mixture before entering the reaction zone. On-line chromatographic analysis was performed using a gas chromatograph equipped with a flame ionization detector and a Bentone 34 packed column (0.6 cm × 1.8 m). Before gas chromatographic analysis, the reaction products were separated and carbon dioxide converted to methane by means of a methanation catalyst (Ni/Kieselghur) operating at 673 K. Benzene and carbon dioxide were the only products detected. The presence of water in the products was verified but not quantified. Carbon monoxide was never detected in the effluent. Before catalytic measurements, all the catalysts were reduced in hydrogen at 673 K for 1 h and then cooled to the desired temperature. The flow of reactants was then started (500 cm^3 min^{-1}). Two experimental procedures were used for catalyst testing. The complete oxidation of benzene was studied by obtaining curves of benzene conversion as a function of temperature (light-off curves). The temperature was raised by steps of about 25 K from 298 to 673 K. More fundamental differential reactor experiments (less than 10% conversion) were performed at constant temperature (<520 K). The products were sampled at 5 min intervals using an automated sampling valve. In these steady-state rate measurements, diffusional limitations were ruled out by varying particle sizes and contact times between 0.15 and 0.49 mm and 5 and 200 g catalyst h mol^{-1} Bz, respectively.

3. Results

3.1. Catalyst characterization

Table 1 shows the Pt and Cl contents, and the metallic dispersions (D_0) of the Pt/Al_2O_3 catalysts used in this work. Catalysts I-A, I-B and F contained about 0.30 wt.% Pt, whereas the platinum loadings

Table 1
Characteristics of Pt/Al_2O_3 catalysts used in this work

Catalyst	Pt loading (wt.%)	Pt dispersion D_0 (%)	Surface Pt concentration (μmol Pt_s g^{-1} catalyst)	Cl concentration (wt.%)
I-A	0.30	65	10.0	0.90
I-B	0.30	37	5.7	0.63
II	0.58	8	2.4	0.58
III	0.52	58	15.5	0.85
F	0.31	51	8.0	0

on catalysts II and III were 0.58 and 0.52 wt.% Pt, respectively. The Pt dispersion on catalysts I-A, III and F, which were not submitted to any sintering treatment, was higher than 50%. The D_0 value on catalyst I-A was substantially higher than on chlorine-free catalyst F, in spite that both catalysts contain similar Pt loadings. This is because catalyst I-A was submitted to a final treatment in a hydroxychlorinating mixture at 773 K to regulate the chlorine level on the support. This treatment simultaneously redisperses the metallic phase because of the formation of surface $[Pt(OH)_4Cl_2]^{2-}$ species showing high surface diffusion mobility [24]. Sintered catalysts I-B and II exhibited lower D_0 values 37 and 8%, respectively. The final sintering treatment at high temperatures in oxygen-containing atmospheres causes the partial elimination of chlorine from the alumina support [25]. As a result, the Cl level on catalysts I-B and II was lower than on fresh catalysts I-A and III.

3.2. Catalytic tests: light-off curves

Fig. 1 shows the X versus T curves obtained on catalysts I-A, I-B and II in two consecutive catalytic tests. On catalyst I-A (Fig. 1a), the reaction started at about 498 K in the first run. The benzene conversion increased then dramatically at ca. 538 K reaching a value of $X \cong 100\%$ between 623 and 673 K. The reaction was maintained at 673 K for 2 h and then the catalyst was purged and cooled down in nitrogen to 373 K. Subsequently, a second catalytic test was carried out. As shown in Fig. 1a, the X versus T curve corresponding to the second run was clearly shifted to lower temperatures as compared to that obtained in the first run. Such a displacement of the light-off curves typically illustrates the catalyst activation phenomenon in hydrocarbon combustion reactions. To compare catalyst activities, we measured from light-off curves, the value of the temperature at $X = 50\%$, $T^{50}_{i,j}$, where i identifies the catalyst and j indicates first (1) or second (2) runs. The difference $\Delta T^{50}_i = T^{50}_{i,1} - T^{50}_{i,2}$, is a measure of the activation phenomenon on catalyst i. The $T^{50}_{\text{I-A},j}$ values are shown in Table 2. It is observed that $T^{50}_{\text{I-A},2}$ was about 56 K lower than $T^{50}_{\text{I-A},1}$. On the other hand, we measured the Pt dispersion on catalyst I-A after the second run (D_2, Table 2). The value of the metallic dispersion on the fresh catalyst ($D_0 = 65\%$) diminished drastically to 9% after the second run.

Similar experiments were carried out on catalysts I-B and II (Fig. 1b and c, respectively). The light-off curves of respective first runs appeared shifted to lower temperatures as compared to that obtained on

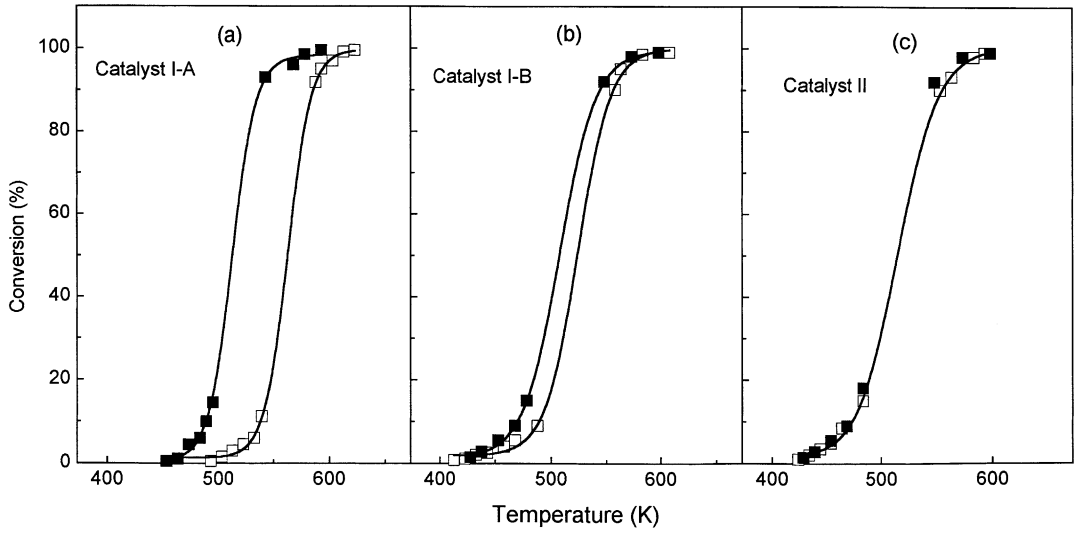

Fig. 1. Consecutive light-off curves for benzene combustion: (□) first run; (■) second run. $W/F^0_{\text{Bz}} = 50$ g catalyst h mol^{-1} Bz, $P = 1$ atm, Bz:O_2:N_2 = 0.65:10:90.

Table 2
Light-off curves[a]

Catalyst	Pt dispersion (%)		Temperatures at $X = 50\%$ (K)		
	D_0[b]	D_2[c]	T_1^{50}	T_2^{50}	ΔT^{50}
I-A	65	9	566	510	56
I-B	35	10	524	505	19
II	8	7	508	508	0
F	50	9	548	513	35

[a] Catalytic activity and Pt dispersion in two consecutive runs ($W/F^0_{Bz} = 50$ g catalyst h mol^{-1} Bz, $P = 1$ atm, Bz:O_2:N_2 = 0.65:10:90).
[b] Pt dispersion of fresh catalysts.
[c] Pt dispersion measured after the second catalytic run.

catalyst I-A. Table 2 shows that both $T^{50}_{\text{I-B},1}$ (524 K) and $T^{50}_{\text{II},1}$ (508 K) were significantly lower than $T^{50}_{\text{I-A},1}$ (566 K). On the other hand, from the consecutive light-off curves on catalysts I-B and II, we measured $\Delta T^{50}_{\text{I-B}} \cong 19$ K and $\Delta T^{50}_{\text{II}} \cong 0$, respectively. This later result shows that the activation phenomenon is not verified on catalyst II. The metallic fraction of fresh catalyst I-B appeared to be severely sintered after two consecutive catalytic tests; the Pt dispersion diminished, in fact, from $D_0 = 35\%$ to $D_2 = 10\%$. On catalyst II, the values of D_0 and D_2 were similar, i.e. about 8%.

To obtain insight on the effect of chlorine on catalyst activation, the oxidation of benzene was also performed on unchlorided catalyst F ($D_0 = 50\%$). Fig. 2 shows that the activation phenomenon takes place on catalyst F; a value of $\Delta T^{50}_{\text{F}} = 35$ K was obtained. The $T^{50}_{\text{F},1}$ and ΔT^{50}_{F} values (Table 2) were both between those measured on catalysts I-A and I-B. After two consecutive catalytic tests, the Pt dispersion of catalyst F diminished from $D_0 = 50\%$ to $D_2 = 9\%$.

The effect of the pretreatment atmosphere on catalyst activation was investigated by heating in situ catalyst I-A at 673 K for 2 h in nitrogen, oxygen, or the reactant feed (0.64% benzene in a 10% O_2/N_2 mixture). Then, a standard catalytic test was performed; results are presented in Fig. 3. The light-off curves obtained on catalyst I-A pretretated in N_2 and O_2 atmospheres were similar; the corresponding $T^{50}_{\text{I-A},1}$ values (∼565 K) were both comparable to that measured from the first run in Fig. 1a. In contrast, the light-off curve on catalyst I-A pretreated in the reactant mixture appeared shifted to lower temperatures and the obtained

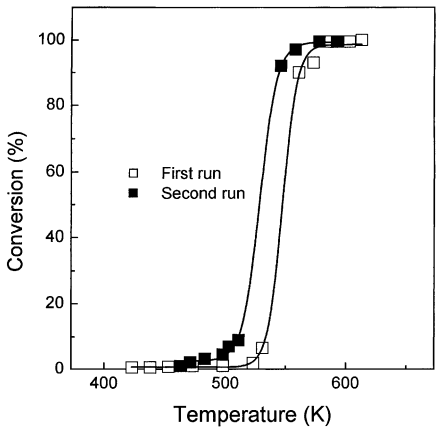

Fig. 2. Consecutive light-off curves on chlorine-free catalyst F. $W/F^0_{Bz} = 50$ g catalyst h mol^{-1} Bz, $P = 1$ atm, Bz:O_2:N_2 = 0.65:10:90.

$T^{50}_{\text{I-A},1}$ value (512 K) was similar to the light-off temperature measured from the second run (Fig. 1a).

Finally, catalyst I-A was submitted to two consecutive catalytic tests, but the standard experimental procedure used for obtaining the X versus T curves of Fig. 1 was changed by reducing the catalyst between the two runs. Specifically, after reaction for 2 h at 673 K at the end of the first run, the system was purged with nitrogen and then catalyst I-A was reduced for 2 h in hydrogen at 673 K. Subsequently, a standard

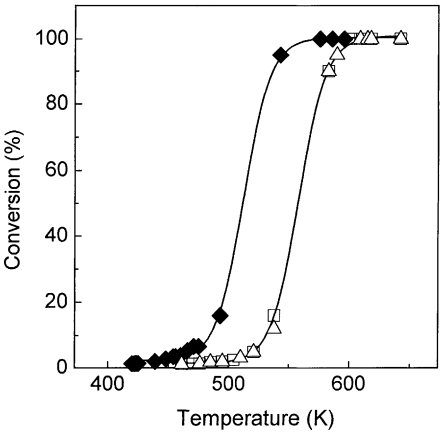

Fig. 3. Effect of the pretreatment atmosphere. Light-off curves obtained after treatment of catalyst I-A at 473 K for 2 h in: (△) nitrogen; (□) oxygen; (◆) reactant mixture.

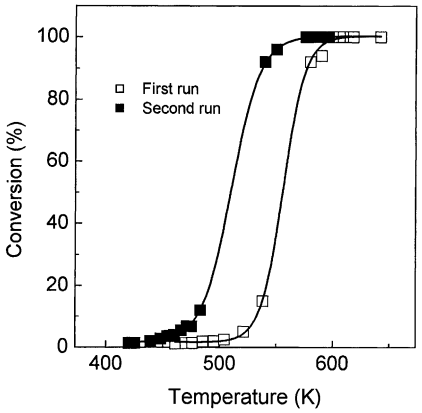

Fig. 4. Consecutive light-off curves on catalyst I-A. The sample was reduced in H_2 at 673 K for 2 h prior to performing the second run.

Table 3
Kinetically-controlled catalytic tests[a]

Catalyst	Pt dispersion (%)		Catalytic activity	
	D_0[b]	D_f[c]	Initial reaction rate, $r_0 \times 10^2$ (mol Bz $h^{-1}\,g^{-1}$ Pt)	Initial TOF (h^{-1})
I-A	65	50	5.0	15
I-B	35	28	21.5	120
II	8	8	31.2	760
III	58	47	5.4	18
F	50	42	6.4	25

[a] Benzene oxidation rates determined from Fig. 5 ($T = 473$ K, $P = 1$ atm, $Bz:O_2:N_2 = 0.22:13:87$).
[b] Pt dispersion of fresh catalysts.
[c] Pt dispersion measured after the 18-h catalytic run.

second catalytic run was carried out. The obtained light-off curves (Fig. 4) were similar to those obtained in Fig. 1a.

3.3. Kinetic-controlled catalytic tests

Benzene oxidation was also carried out on platinum catalysts at constant temperatures between 453 and 523 K. In all the cases, the initial conversion was lower than 10% and the reaction was kinetically controlled. Fig. 5 shows the X versus time curves obtained at 473 K, and typically illustrates the time-on-stream behavior of the catalysts during the reaction. The activities of catalysts I-A, I-B, III and F at 473 K slowly increase with time along the 18-h run, while the benzene conversion on catalyst II remains approximately constant. After the catalytic tests of Fig. 5, the metallic dispersion of the samples were measured by hydrogen chemisorption; the obtained values are given in Table 3. It is observed that, excepting for catalyst II, the metallic dispersion diminished during the 18-h run. In order to further investigate Pt particle size changes during reaction, we examined the metallic fraction of sample III before and after the catalytic test by TEM. Fig. 6 compares micrographs of both samples and shows that the Pt crystallites, which are not detected on the fresh sample, are clearly observed on the spent catalyst.

Fig. 7 shows the X versus time curves obtained on catalyst I-A at three temperatures 493, 503 and 518 K. It is observed that at 503 and 518 K, the reaction ignites before ending the 18-h run. Following a slow initial increase of the catalyst activity, both the benzene conversion and the temperature abruptly increase and the reaction cannot be longer controlled in low conversion regimes. Qualitatively, a similar activation phenomenon was observed on catalyst I-B. In contrast, the initial activity of catalyst II did

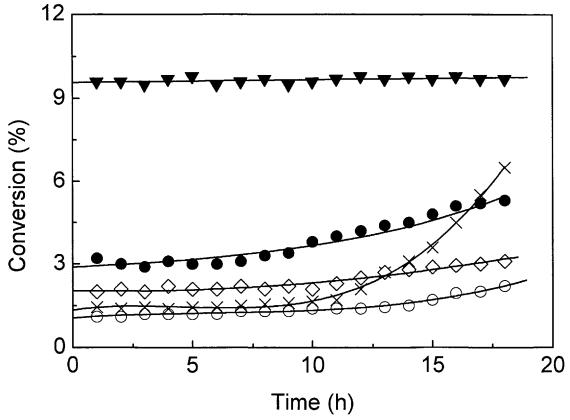

Fig. 5. Benzene conversion as a function of time: catalysts I-A (○); I-B (●); II (▼); III (×) and F (◇). $T = 473$ K, $P = 1$ atm, $Bz:O_2:N_2 = 0.22:13:87$. W/F^0_{Bz} was 50 g catalyst h mol^{-1} Bz for catalysts I-B, II, and III, and 110 g catalyst h mol^{-1} for catalysts I-A and F.

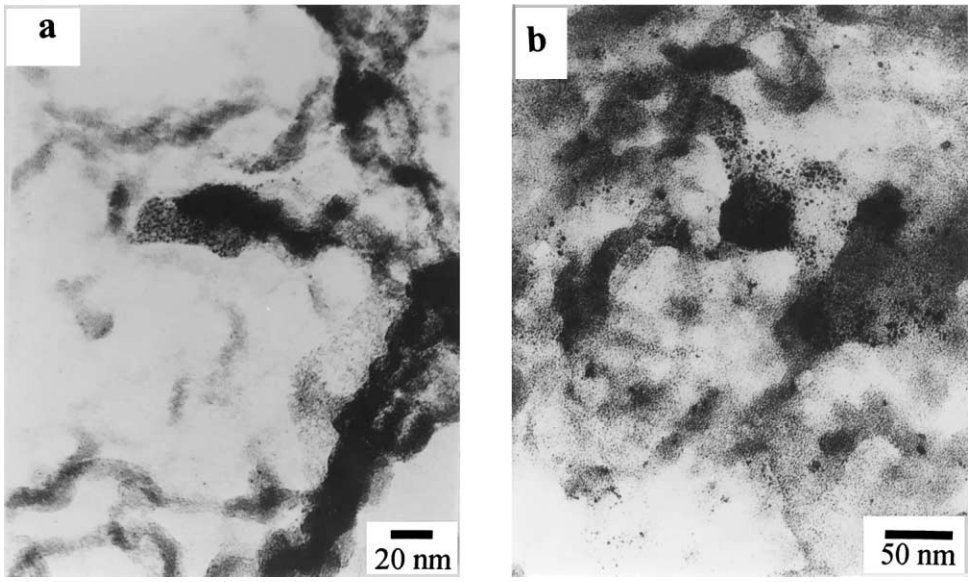

Fig. 6. TEM micrographs of catalyst III: (a) fresh sample; (b) sample recovered after the catalytic test of Fig. 5.

not change with time in the 453–523 K temperature range.

To compare intrinsic catalyst activities, we calculated from Fig. 5 the initial TOF (h^{-1}) at 473 K; the values are shown in Table 3. The TOF decreased with D_0 in the Pt dispersion range investigated; the TOF value on catalyst II ($D_0 = 8\%$) was about 50 times higher than that measured on catalyst I-A ($D_0 = 65\%$).

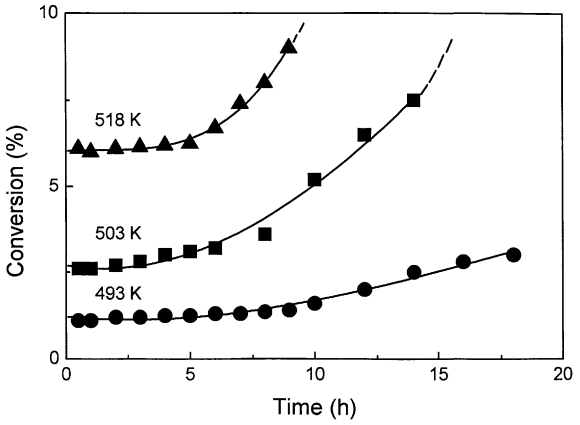

Fig. 7. Benzene conversion on catalyst I-A as a function of time. $W/F^0_{Bz} = 115\,g$ catalyst $h\,mol^{-1}$ Bz, $P = 1$ atm, $Bz{:}O_2{:}N_2 = 0.22{:}13{:}87$.

The reaction orders on catalysts I-A and II were determined by considering for initial reaction rate r_0 (mol Bz $h^{-1}\,g^{-1}$ Pt), a power-law rate equation

$$r_0 = k(P^0_{Bz})^{\alpha}(P^0_{O_2})^{\beta}$$

where P^0_{Bz} and $P^0_{O_2}$ are the partial pressures of benzene and oxygen in the feed, respectively. The α-values were measured by varying the benzene partial pressure between 0.2×10^{-3} and 0.64×10^{-3} atm at a fixed oxygen pressure (0.13 atm). Similarly, reaction order β was obtained by varying $P^0_{O_2}$ between 0.08 and 0.15 atm while keeping P^0_{Bz} at 0.2×10^{-3} atm. In Fig. 8, the r_0 values obtained on catalysts I-A and II were represented as a function of P^0_{Bz} and $P^0_{O_2}$ in logarithmic plots. Reaction orders α and β were determined graphically from Fig. 8. On both catalysts, we measured $\alpha \cong 0$ and $\beta \cong 1$. In Fig. 9, we plotted the ln TOF values as a function of $1/T$ for calculating the apparent activation energy (E_a) and the pre-exponential factor A of benzene combustion on catalysts I-A and II via an Arrhenius-type function. From the slope of the resulting linear plots, we obtained E_a values of 18 ± 1 kcal mol^{-1} on both catalysts, and from the ordinate values at $1/T = 0$, we determined an $A_{II}/A_{I\text{-}A}$ ratio of about 70.

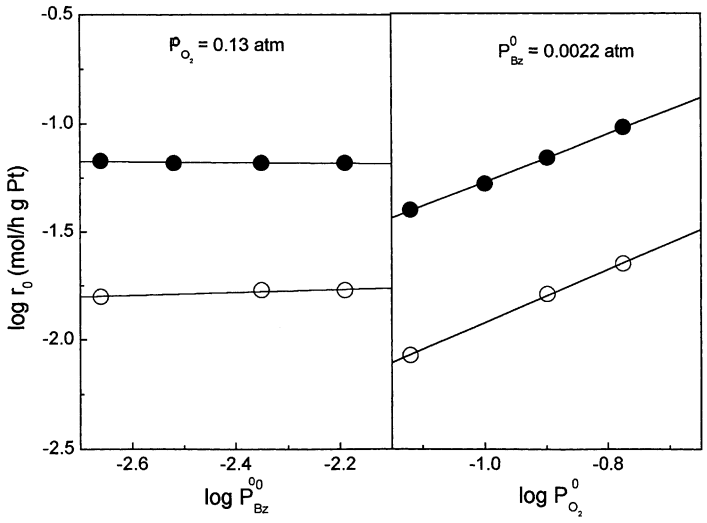

Fig. 8. Dependence of the benzene oxidation reaction upon benzene and oxygen partial pressure. Catalyst I-A (○); catalyst II (●). $T = 443$ K, $P = 1$ atm.

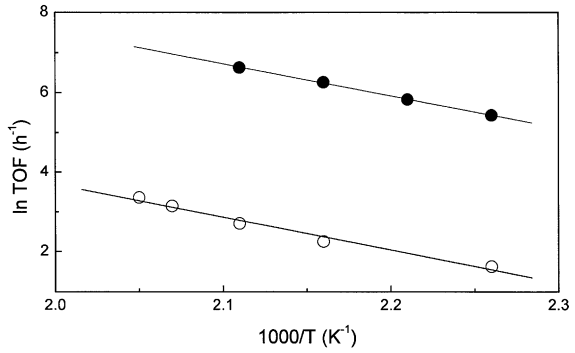

Fig. 9. Arrhenius plots for determining E_a (apparent activation energy) and A (pre-exponential factor). Benzene oxidation turnover rates as a function of inverse temperature on catalysts I-A (○) and II (●). $W/F^0_{Bz} = 115$ g catalyst h mol^{-1} Bz, $P = 1$ atm, $Bz:O_2:N_2 = 0.22:13:87$.

4. Discussion

4.1. Effect of Pt dispersion on benzene oxidation turnover rates

Fig. 1 and Table 2 show that the light-off curves corresponding to first runs are shifted to lower temperatures with increasing Pt particle size. The T_1^{50} values diminished from 566 K on catalyst I-A ($D_0 = 65\%$) to 508 K on catalyst II ($D_0 = 8\%$). Kinetically-controlled catalytic tests confirmed the effect of Pt particle size on benzene combustion activity. In fact, from data in Table 3, it is inferred that in the Pt dispersion range studied the turnover rates measured from low-conversion catalytic tests increased exponentially with Pt crystallite size. This result shows that benzene combustion on Pt/Al_2O_3 catalysts is a structure-sensitive reaction preferentially promoted on larger Pt crystallites.

Results in Figs. 8 and 9 show that both the reaction orders and the apparent activation energy do not change significantly with changing the metallic dispersion. Benzene combustion turnover rate on catalyst II is about 50 times greater than on catalyst I-A and this difference is clearly beyond the difference in reaction rates which can be caused for experimental errors in determining E_a. The higher activity exhibited by low-dispersed Pt catalysts is not caused, therefore, by a change in the combustion reaction mechanism. In contrast, the pre-exponential factor A measured on catalyst II was clearly higher than that obtained on catalyst I-A thereby suggesting that the density of active sites changes with increasing Pt particle size. Our kinetic results may be interpreted by considering that the benzene oxidation on platinum occurs via the

simplified Langmuir–Hinshelwood mechanism proposed by Barresi and Baldi [9,26]. To account for the observed benzene zero-order reaction, these authors proposed that benzene and oxygen are adsorbed on different sites and that the rate of oxygen adsorption is very low compared to the rate of benzene adsorption. The mechanism may be represented by the following elementary steps:

$$O_2 + L \underset{\text{slow}}{\overset{k_1}{\rightarrow}} O_2 \cdot L \underset{\text{very fast}}{\overset{+L}{\rightarrow}} 2O \cdot L \quad r_1 = k_1 P_{O_2} C_L \tag{1}$$

$$Bz + L' \leftrightarrows Bz \cdot L'$$
$$K_1 = \frac{C_{Bz\cdot L'}}{P_{Bz} C_{L'}} \tag{2}$$

$$Bz \cdot L' + O \cdot L \overset{k_2}{\rightarrow} (I) \rightarrow \text{products}$$
$$r_2 = k_2 C_{Bz\cdot L'} C_{O\cdot L} \tag{3}$$

where L and L′ represent the adsorption sites for oxygen and benzene, respectively, and (I) a generic intermediate, k_1 the kinetic constant of oxygen chemisorption and k_2 the kinetic constant of the elementary step determining the rate of the surface reaction. In agreement with previous work dealing with the adsorption of benzene on supported and unsupported Pt [27,28], the above mechanism assumes that benzene is rapid and strongly adsorbed on the metallic Pt sites. Benzene adsorbs by a π-bond interaction in which the ring lies parallel to the metal surface [29,30]. The adsorption kinetics of oxygen on metal Pt atoms is assumed to be relatively slow, but the chemisorbed molecular oxygen is quickly decomposed into atomic oxygen so that the surface concentration of molecular oxygen is negligible. The two adsorption sites model may be justified by assuming for the active platinum surface a model similar to that proposed for hydrogenation [31,32]. The model assumes that the surface is mostly covered with a partially dehydrogenated carbonaceous layer that leaves islands of accessible platinum clusters for dissociative, non-competitive O_2 adsorption. From the above elementary steps, the expression of initial rate r_0 results:

$$r_0 = \frac{k_1 k_2 K_1 C_T C_{T'} P_{O_2} P_{Bz}}{\nu k_2 K_1 C_{T'} P_{Bz} + k_1 P_{O_2} (1 + K_1 P_{Bz})} \tag{4}$$

where ν is the stoichiometric coefficient of oxygen in the overall reaction ($\nu = 7.5$ for benzene combustion), and C_T and $C_{T'}$ the total site concentrations available for benzene and oxygen adsorption, respectively. If $k_1 \ll k_2$, Eq. (4) reduces to

$$r_0 = \frac{k_1 C_T P_{O_2}}{\nu} \tag{5}$$

and the orders with respect to benzene and oxygen predicted by Eq. (5) are 0 and 1, respectively, which are the approximate orders determined from our experiments. An apparent zero-order reaction with respect to the hydrocarbon has been previously reported for the oxidation of different aromatic hydrocarbons (namely benzene, toluene, *o*-xylene, ethylbenzene) over platinum-based catalysts [7,26,33]. In contrast, an apparent first-order reaction in oxygen has been observed only with benzene [9]. It is noteworthy that the oxidation of methane on Pt-based catalysts is first-order in the hydrocarbon and zero-order in oxygen [16,34,35]. This suggests that the reaction of oxygen with benzene proceeds through a different mechanism than with methane. For methane oxidation, it is widely accepted that the initial activation of the hydrocarbon, i.e. the first hydrogen subtraction from adsorbed methane with chemisorbed oxygen, is the rate-limiting step for the overall combustion process [15,16]. For benzene combustion, Eq. (5) is the limiting form of Eq. (4) and is obtained when the rate constant for oxygen adsorption on platinum (k_1) is very low compared to the rate constant of the surface reaction (k_2). Any increase in rate constant k_1 accelerates, in this case, the benzene oxidation rate. Our results show that by diminishing the Pt dispersion the apparent activation energy for benzene oxidation reaction does not change but the pre-exponential factor A clearly increases. The observed turnover rate increase with increasing Pt particle size would reflect, therefore, an increase in the density of reactive Pt–O species resulting from higher Pt oxidation rates. Duprez [36] studied the effect of the particle size on the adsorption/desorption rate of oxygen on Rh, Pd and Pt by $^{18}O_2$ isotopic exchange techniques. He found that the $^{18}O_2 + {}^{16}O_2$ equilibration turnover rate increases more than two-orders when the Pt dispersion is decreased from 57 to 4%. The effect of particle size on the reactivity of oxygen-adsorbed Pt supported on alumina was studied by Briot et al. [17].

These authors reported that on larger Pt crystallites the heat of oxygen chemisorption decreases and the reactivity of chemisorbed oxygen increases. The lower reactivity of very small oxidized Pt particles toward hydrogen was observed by several authors [37,38]. In well-dispersed platinum-supported catalysts, platinum is completely oxidized to PtO_2 when treated in oxygen at temperatures higher than 473 K [39]. However, McCabe et al. [38] reported that only the surface of large Pt crystallites is oxidized during heating in air up to 873 K. In recent studies using X-ray absorption spectroscopy (EXAFS), we investigated the Pt–O interaction on fresh and sintered Pt/Al_2O_3 catalysts following the sample oxidation in oxygen at 573 K [40]. We found that on sintered catalysts, the Pt–Pt coordination increases, while the Pt–O coordination decreases as compared with fresh catalysts. The structural information supplied by EXAFS showed that the oxidation of large Pt crystallites involves only the outermost metal shell. This passivation coating is formed of a surface layer of PtO_6 octahedra which corresponds to the crystallographic arrangement in bulk PtO_2. Based on similar evidences, Hicks et al. [5] considered that by increasing the Pt particle size the interaction of oxygen with platinum goes from a "surface oxide" to a "chemisorbed layer" oxygen species. All these results are consistent with the assumption that the number of Pt–O bonds of lower binding energy, i.e. the site density of more reactive surface oxygen, increases on larger Pt particles.

4.2. Effect of Pt dispersion on initial activation periods

Fig. 1 shows that on chlorided Pt/Al_2O_3 catalysts of high metallic dispersion (catalysts I-A and I-B) the light-off curves are shifted to lower temperatures after a first catalytic test. Unchlorided catalyst F exhibited a similar qualitative shift of the consecutive light-off curves (Fig. 2), thereby indicating that the observed catalyst activation phenomenon is not caused by the presence of chlorine on the support. On the other hand, our results suggest that catalyst I-A is activated in situ during the reaction. As shown in Fig. 3, the *X* versus *T* curve obtained on catalyst I-A following a catalyst pretreatment in the reactant mixture at 673 K for 2 h appears clearly shifted to lower temperatures as compared to those curves obtained after similar pretreatments in nitrogen or oxygen atmospheres. From the results in Fig. 4, we can exclude that the initial catalyst activation is caused by formation of Pt^{n+} surface species during reaction. Fig. 4 shows, in fact, that the light-off curve shifts to lower temperatures in spite of reducing catalyst I-A in H_2 at 673 K for 2 h before performing the second catalytic test. In summary, the above results show that well-dispersed Pt catalysts are activated on stream, but not because of the in situ formation of oxidized or oxychlorided Pt^{n+} species. This is consistent with previous reports postulating that platinum remains in zero valence state throughout catalytic oxidation of hydrocarbons [15].

The metallic fraction of well-dispersed Pt/Al_2O_3 catalysts appeared severely sintered after two consecutive *X* versus *T* tests; for example, the Pt dispersion of catalyst I-A dropped from $D_0 = 65\%$ to $D_2 = 9\%$ (Table 2). In contrast, on low-dispersed Pt catalysts the consecutive light-off curves are similar and the metallic dispersion is not modified (results for catalyst II in Fig. 1c and Table 2). The dependence of the activation phenomenon with the platinum dispersion is confirmed by the results obtained from kinetically-controlled catalytic tests (Figs. 5 and 7). In fact, Fig. 5 shows that while the benzene conversion increases with time on well-dispersed Pt catalysts, the activity of catalyst II does not change on stream. On the other hand, TEM characterization (Fig. 6) and hydrogen chemisorption measurements (Table 3) showed that the increase of the benzene conversion with time parallels a concomitant increase in the Pt particle size. The general picture emerging from the above results is that the initial activation of well-dispersed Pt catalysts is caused by the sintering of the metallic phase, which occurs on stream even if the reaction is performed at low-temperature and low-conversion regimes. Benzene oxidation is highly exhotermic ($-\Delta H = 781\,\text{kcal mol}^{-1}$) and the Pt crystallite temperature is significantly increased during reaction. Hot-spots on the metallic particles together with the presence of gaseous water cause the metal phase sintering and the formation of larger, more active, Pt particles. As a result, the benzene conversion increases with time until the formation of larger steady state Pt particles is completed. This explains the existence of initial activation periods on well-dispersed Pt/Al_2O_3 catalysts for the benzene oxidation reaction.

Marceau et al. [14] studied the oxidation of methane at 723 K on chlorided and unchlorided Pt/Al_2O_3 catalysts and observed that on chlorided samples the activity increases with time concomitantly with chlorine elimination from the support. Based in previous work showing that chlorine may block the active sites for alkane oxidation on Pd [41] and Pt [13], they concluded that the elimination of chlorine on stream increases the accessibility of reactant gases to metallic Pt sites and as a result the activity increases. However, our results suggest that the role of chlorine, if any, is not significant for explaining the existence of initial activation periods for benzene oxidation on platinum catalysts. In fact, Fig. 6 shows that, as on well-dispersed chlorided Pt catalysts, the activity for benzene combustion increases with time on chlorine-free sample F, i.e. the activation phenomenon takes place irrespective of the presence of chlorine on the catalysts. The induction periods are not caused, therefore, by the presence of chlorided ions on the catalyst but by the sintering of the Pt crystallites.

5. Conclusions

The main conclusions of this study regarding the structure sensitivity and in situ activation of benzene combustion on Pt/Al_2O_3 catalysts are summarized as follows:

1. The oxidation of benzene on Pt/Al_2O_3 catalysts is a structure-sensitive reaction preferentially promoted on larger metallic particles. Kinetic results are well interpreted by assuming that the reaction occurs via a Langmuir–Hinshelwood mechanism, being the rate constant of oxygen adsorption on Pt very low as compared to that of the surface reaction step. Increasing the Pt particle size increases the density of reactive Pt–O species but does not modify the reaction mechanism.
2. The activity of well-dispersed Pt/Al_2O_3 catalysts increases with time, irrespective of the chlorine level on the sample. The existence of initial activation periods is caused by sintering of the metallic phase on stream. Hot-spots on the metallic particles together with the presence of gaseous water in the products cause the formation of larger, more reactive, platinum crystallites, even at mild reaction conditions. Steady-state conditions are reached when the rate growth of Pt particles is negligible because of the formation of very large metallic particles (in the range corresponding to platinum dispersions lower than 10%).

Acknowledgements

We acknowledge P. Reyes (Universidad de Concepción, Chile) for carrying out sample characterization by TEM. We are grateful to E. Rincón for his participation in some of the catalytic experiments. We thank the Consejo Nacional de Investigaciones Científicas y Técnicas (CONICET), Argentina, and the Universidad Nacional del Litoral, Santa Fe, Argentina, for financial support.

References

[1] J.J. Spivey, Ind. Eng. Chem. Res. 26 (1987) 2165.
[2] W. Chu, H. Windawi, Chem. Eng. Prog. (1996) 37.
[3] J.H. Lee, D. Trimm, Fuel Proc. Technol. 42 (1995) 339.
[4] R.J. Farrauto, M.C. Hobson, T. Kennelly, E.M. Waterman, Appl. Catal. A 81 (1992) 227.
[5] R.F. Hicks, H. Qi, M.L. Young, R.G. Lee, J. Catal. 122 (1990) 280.
[6] F.H. Ribeiro, M. Chow, R.A. Dalla Beta, J. Catal. 146 (1994) 277.
[7] K.T. Chuang, S. Cheng, S. Tong, Ind. Eng. Chem. Res. 31 (1992) 2466.
[8] J. Hermia, S. Vigneron, Catal. Today 17 (1993) 349.
[9] A.A. Barresi, G. Baldi, Ind. Eng. Chem. Res. 33 (1994) 2964.
[10] P. Papaefthimiou, T. Ioannides, X.E. Verykios, Appl. Catal. B: Environ. 13 (1997) 175.
[11] R. Burch, P.K. Loader, F.J. Urbano, Catal. Today 27 (1996) 243.
[12] K. Fujimoto, F. Ribeiro, H.M. Avalos Borja, E. Iglesia, J. Catal. 179 (1996) 431.
[13] P. Marécot, A. Fakche, B. Kellali, G. Mabilon, M. Prigent, J. Barbier, Appl. Catal. B: Environ. 3 (1994) 283.
[14] E. Marceau, M. Che, J. Saint-Just, J.M. Tatibouët, Catal. Today 29 (1996) 415.
[15] M. Aryafar, F. Zaera, Catal. Lett. 48 (1997) 173.
[16] K. Otto, Langmuir 5 (1989) 1364.
[17] P. Briot, A. Auroux, D. Jones, M. Primet, Appl. Catal. 59 (1990) 141.
[18] M. Kobayashi, T. Kanno, A. Konishi, H. Takeda, React. Kinet. Catal. Lett. 37 (1988) 89.
[19] V. Labalme, E. Garbowsky, N. Ghilhaume, M. Primet, Appl. Catal. A: Gen. 138 (1996) 93.
[20] R.F. Hicks, R.G. Lee, W.J. Han, A.B. Kooh, in: R.K. Graselli, W. Sleight (Eds.), Structure–Activity and Selectivity Relationship in Heterogeneous Catalysis, Elsevier, Amsterdam, 1991, p. 127.

[21] C. Pliangos, I.V. Yentekakis, V.G. Papadakis, C.G. Vayenas, X.E. Verykios, Appl. Catal. B: Environ. 14 (1997) 161.
[22] P. Papaefthimiou, T. Ioannides, X.E. Verykios, Appl. Catal. B: Environ. 15 (1998) 75.
[23] G. Dalmai-Imelik, C. Leclercq, I. Mutin, J. Micro Spectrosc. Electron 20 (1974) 123.
[24] F. Le Normand, A. Borgna, T.F. Garetto, C.R. Apesteguía, B. Moraweck, J. Phys. Chem. 100 (1996) 9068.
[25] A. Borgna, T.F. Garetto, C.R. Apesteguía, F. Le Normand, B. Moraweck, J. Catal. 186 (1999) 433.
[26] A.A. Barresi, G. Baldi, Chem. Eng. Sci. 47 (1992) 1943.
[27] J.A. Brundege, G. Parravano, J. Catal. 2 (1963) 380.
[28] S.D. Lin, M.A. Vannice, J. Catal. 143 (1993) 143.
[29] T.E. Fischer, S.R. Kelemen, H.P. Bonzel, Surf. Sci. 64 (1977) 157.
[30] M. Surman, S.M. Bare, P. Hofmann, D.A. King, Surf. Sci. 126 (1983) 349.
[31] G.A. Somorjai, Adv. Catal. 26 (1977) 1.
[32] S.D. Linn, A.M. Vannice, J. Catal. 143 (1993) 563.
[33] S.K. Gangwal, M.E. Mullins, J.J. Spivey, P.R. Caffrey, Appl. Catal. 36 (1988) 231.
[34] Y.F.Y. Yao, Ind. Eng. Chem. Prod. Res. Dev. 5 (1980) 293.
[35] M. Niwa, K. Awano, Y. Murakami, Appl. Catal. 7 (1983) 317.
[36] D. Duprez, in: C. Li, Q. Xin (Eds.), Studies in Surface Science and Catalysis, Vol. 112, Elsevier, Amsterdam, 1997, p. 13.
[37] H.C. Yao, M. Sieg, H.K. Plummer, J. Catal. 59 (1979) 365.
[38] R.W. McCabe, C. Wong, H.S. Woo, J. Catal. 144 (1988) 354.
[39] H. Lieske, G. Lietz, H. Spindler, J. Volter, J. Catal. 81 (1983) 8.
[40] A. Borgna, F. Le Normand, T. Garetto, C.R. Apesteguía, B. Moraweck, Catal. Lett. 13 (1992) 175.
[41] D.O. Simone, T. Kennelly, N.L. Brungard, R.J. Farrauto, Appl. Catal. 70 (1991) 87.